Swansea University
Prifysgol Abertawe

Cronfa
Setting Research Free

Cronfa - Swansea University Open Access Repository

This is an author produced version of a paper published in:
Nanotechnology

Cronfa URL for this paper:
http://cronfa.swan.ac.uk/Record/cronfa38951

Paper:

http://www.swansea.ac.uk/library/researchsupport/ris-support/

Investigation into the Effects of Surface Stripping ZnO Nanosheets

Chris J. Barnett*[1,], Georgina Jackson[2], Daniel R. Jones[1], Aled R. Lewis[3], Kathryn Welsby[2], Jon E. Evans[3], James D. McGettrick[3], Trystan Watson[3], Thierry G. G. Maffeis[3], Peter R. Dunstan[2], Andrew R. Barron[1,4,5] and Richard J. Cobley[3]

1   Energy Safety Research Institute, Swansea University, Bay Campus, Swansea SA1 8EN, U.K.

2   Department of Physics, College of Science, Swansea University, Singleton Park, Swansea SA2 8PP, U.K.

3   College of Engineering, Swansea University, Bay Campus, Swansea SA1 8EN, U.K.

4   Department of Chemistry, Rice University, Houston, Texas 77005, U.S.A.

5   Department of Materials Science and Nanoengineering, Rice University, Houston, Texas 77005, U.S.A.

c.j.barnett@swansea.ac.uk, 741330@swansea.ac.uk, d.r.jones@swansea.ac.uk, 557952@swansea.ac.uk, k.a.welsby@swansea.ac.uk, j.e.evans@swansea.ac.uk, j.d.mcgettrick@swansea.ac.uk, t.m.watson@swansea.ac.uk, t.g.g.maffeis@swansea.ac.uk, p.r.dunstan@swansea.ac.uk, a.r.barron@swansea.ac.uk, richard.j.cobley@swansea.ac.uk.

Keywords: ZnO, Nanosheets, Argon, XPS, Ohmic, Schottky, Photoluminescence, Conduction

Abstract

ZnO nanosheets are polycrystalline nanostructures that are used in devices including solar cells and gas sensors. However, for efficient and reproducible device operation and contact behaviour the conductivity characteristics must be controlled and surface contaminants removed. Here we use low doses of argon bombardment to remove surface contamination and make reproducible lower resistance contacts. Higher doses strip the surface of the nanosheets altering the contact type from near-ohmic to rectifying by removing the donor-type defects, which PL shows to be concentrated in the near-surface. Controlled doses of argon treatments allow nanosheets to be customised for device formation.

Introduction

Zinc Oxide (ZnO) is a wide band gap (3.37 eV) metal oxide piezoelectric semiconductor that has the ability to be formed in numerous nanostructures including nanowires, nanorods and nanosheets [1-3]. Due to their high surface area to volume ratio, polycrystalline ZnO nanosheets have been shown to have potential practical application in gas-sensing devices and dye-sensitised solar cells [4-6].

These devices require surface contamination to be removed in order to create a consistent contact. One method of doing this involves annealing the nanosheets; however, previous work has shown that vacuum annealing causes changes in the polycrystalline structure and to the defect chemistry, which affects the conduction characteristics of the nanosheets [7].

Other commonly used methods to clean nanostructures are plasma treatments and argon bombardment [8-10]. Argon plasma treatment has been observed to increase the mobility, carrier concentration and conductivity of ZnO nanowires [11] and has been used by Dulub et al. [12] to clean single crystal ZnO in order to carry out scanning tunnelling microscopy (STM). Our previous work found that argon bombardment using 0.3 kV for 20 minutes on ZnO nanowires removed surface contamination resulting in a more consistent contact and a three orders of magnitude drop in resistance due to the reduced contact resistance [13]. It was also found that higher powered argon bombardment (1-2.5 kV for 20 minutes) stripped the surface resulting in a reduction in the number of defects observed using photoluminescence (PL). This indicated that the reduction in donor states caused the formation of a more rectifying contact and suggested that the defects are situated at the near-

surface of ZnO nanorods. It is not known whether the defects of polycrystalline ZnO are situated in the near-surface and can be stripped using argon bombardment in order to control the conductivity and contact type.

Here we investigate the effects of argon bombardment on the conduction characteristics and chemistry of polycrystalline ZnO nanosheets using scanning electron microscope (SEM), X-ray photoelectron spectroscopy (XPS), two-point probe and PL.

Method

Layered basic zinc acetate (LBZA) nanosheets were synthesised in an 800 W commercial microwave in a 500 ml solution of 0.1 M zinc acetate dihydrate ($Zn(CH_3COO)_2.2H_2O$) and 0.04 M hexamethylenetetramine (HMTA, $(CH_2)_6N_4$) for 6 mins [6]. The solution was then centrifuged, the supernatant removed and the residue re-suspended in DI water. The LBZA nanosheets were then deposited on n-type (100) silicon and annealed in air at 400 °C to thermally decompose the LBZA into ZnO. Thirteen samples were made in this way.

An Omicron LT nanoprobe equipped with a PSP ISIS 3000 ion gun was used to argon bombard the samples. One sample was loaded into the system but not treated with argon to act as a control, hereafter known as the 'before' sample. The remaining 12 samples were subjected to various argon treatments at room temperature using energies of 0.3, 1.0 and 2.0 keV for time lengths ranging between 5 and 20 minutes.

Nanoscale two-point probe measurements were performed using tungsten probes that had been annealed to reduce probe oxide contamination [14, 15] and approached using a method to ensure minimal compressive strain at the point of contact providing intrinsic characterisation [16]. Five I-V repeat sweeps were performed between potential differences of -2 V and 2 V on randomly selected nanosheets and the probe separation was varied. All measurements were carried out at room temperature.

Surface chemical characterisation was carried out using a Kratos AXIS Supra XPS, Hitachi S4800 SEM and PL measurements obtained through use of a 325-nm wavelength He-Cd laser and an Ocean Optics USB2000+ spectrometer. For the XPS, three areas of the samples were scanned using a monochromatic Al K_α X-ray source and a charge neutraliser, with spectra measured at a pass energy of 20 eV. In the case of the PL measurements, three

spectra were acquired at room temperature from different areas of the sample and then normalised and averaged.

Results and Discussion

The synthesised ZnO nanosheets were of rectangular form with lengths typically ranging from 1 to 20 μm and widths of 1 to 15 μm, which is in general agreement with our previous results [7]. Figure 1 shows a SEM image of the grain structure of a typical ZnO nanosheet before argon bombardment, Figure S1 in the supplemental information shows the nanosheet coverage of the sample. The average grain size was 5 nm and the surface consisted of voids and uneven features.
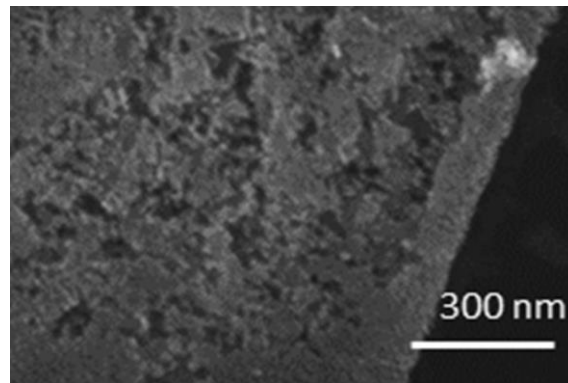
Figure 1: SEM image of ZnO nanosheet before argon bombardment.
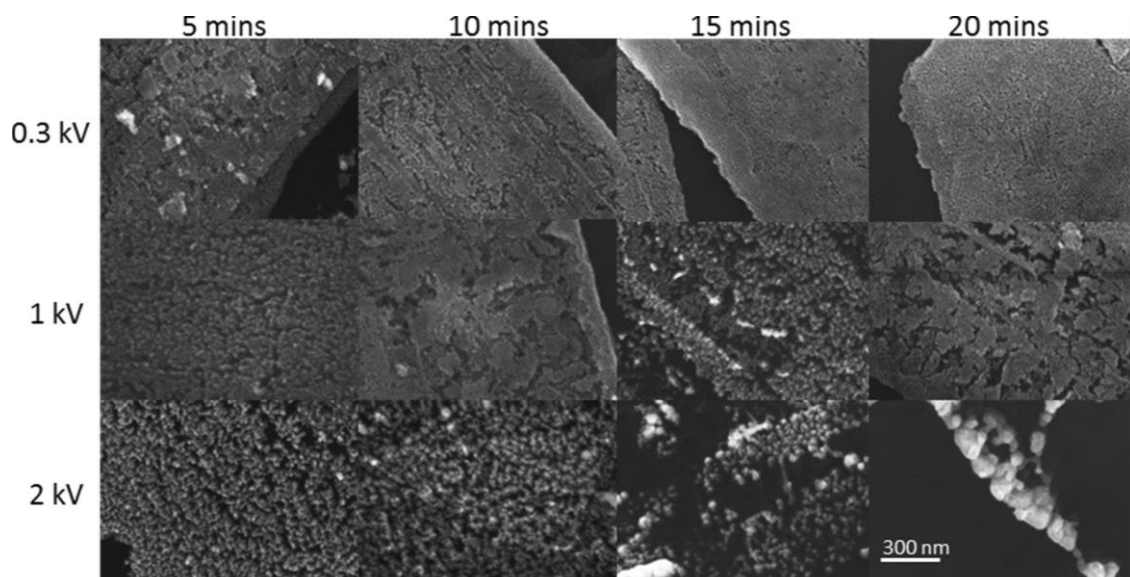
Figure 2: SEM images of ZnO nanosheets after argon bombardment of 0.3 kV, 1 kV and 2kV for time durations 5, 10, 15 and 20 minutes.

Figure 2 shows SEM images of samples subjected to argon bombardment. Argon bombardment at 0.3 kV caused no observable change to the structure of the ZnO nanosheets while bombardment at 1 kV caused observable damage to the ZnO nanosheets by stripping the surface causing the silicon substrate to be visible under the nanosheets. Bombardment at 2 kV also caused observable damage to the nanosheets, with bombardment of duration greater than 15 mins resulting in the nanosheets being almost completely destroyed.

XPS scans were recorded to assess whether the argon bombardment had had an effect on the surface chemistry, including a survey spectrum and detailed spectra of the Zn 2p, Zn 3p, O 1s, Ar 2p and C 1s core levels and Zn LMMA. Figure 3 shows the changes in the survey scan, Zn 2p core level and the Zn LMMA scans following argon bombardment at different powers and times, and the O 1s fit. The survey spectrum shows a peak at 99.4 eV, which is associated with Si from the silicon dioxide substrate. Analysis of the C 1s peak revealed that the quantity of carbon varied randomly with bombardment dose, which we attribute to the random distribution of carbon throughout the ZnO nanosheet structure resulting from the incomplete oxidation of zinc acetate during the annealing. This meant that analysis of carbon contamination removal due to the argon bombardment was not possible.
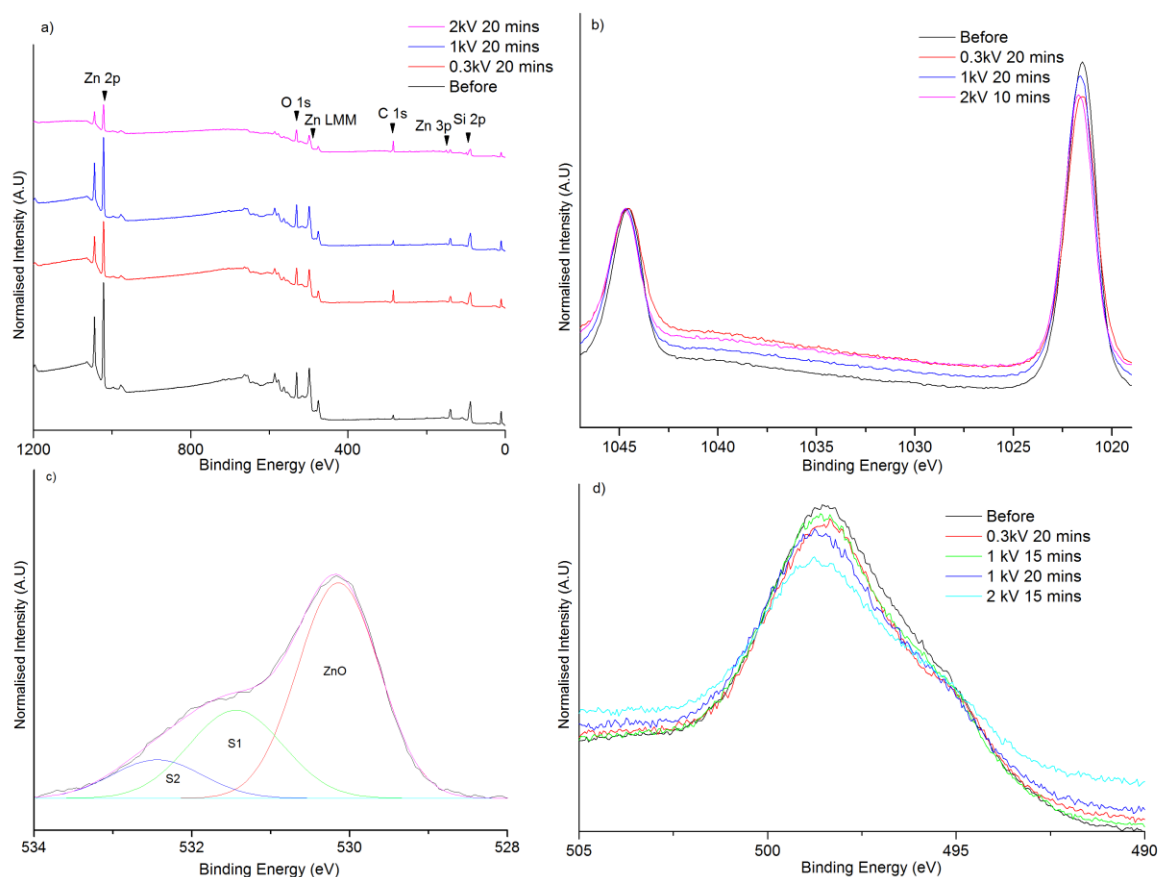
Figure 3. a) Evolution of the survey scan with argon bombardment dose, b) Evolution of the Zn 2p peak with argon bombardment, c) The O 1s peak before argon bombardment, showing fits and background and d) Evolution Zn LMMA peak with argon bombardment.

There was no significant change in the Zn 3p or 2p peaks with argon bombardment; however, it is known these peaks are almost independent of the type of chemical bonds [17].

Before argon bombardment, the O 1s peak consisted of a main component centred at 530.2 eV, and a shoulder on the higher binding energy side consisting of two peaks offset from the main component by 1.35 eV and 2.3 eV, labelled as S1 and S2, respectively. These peaks are attributed to lattice oxygen, surface hydroxide ions and surface water vapour, respectively [18-22]. Curve fitting area analysis of these peaks was used to calculate the percentage water vapour component contribution to the O 1s peak and the results are show in Figure 4a). Since the C 1s spectrum was not a suitable measure of surface contamination, the S2 component was used instead. The quantity of water measured decreased with both increased acceleration voltage and bombardment time; it was also noted that the S1 component followed similar trends.

6
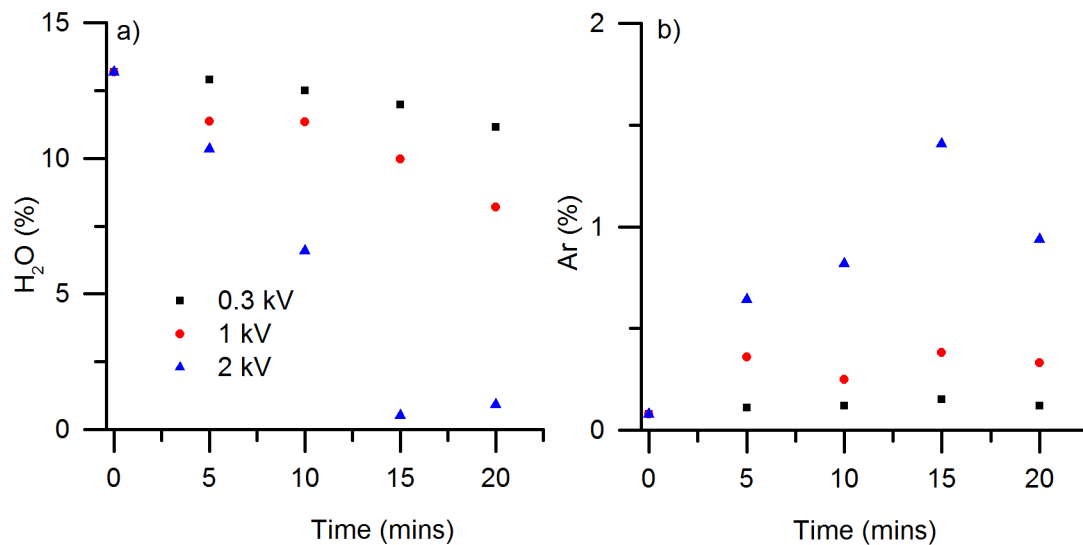
Figure 4: Plots of a) Percentage H₂O and b) Argon against time of argon bombardment.

It is known that high energy ion bombardment can cause argon to be incorporated into the sample [23], and the Ar 2p spectra was therefore also fitted. Figure 4b) depicts the percentage Ar measured in each sample and shows that there was no increase in argon incorporated into the ZnO nanosheets by argon bombardment at 0.3 kV as the quantity measured is not above the background noise of argon measured from the "before" sample. However, when an acceleration voltage of greater than 1 kV was used, an increased quantity of argon was measured compared to the untreated sample.

The Zn LMMA peak, depicted in Figure 3d), is consistent with that of ZnO and did not alter shape with argon bombardment at 0.3 kV and up to 15 mins at 1 kV. After the nanosheets were bombarded for 20 mins at 1 kV and at 2 kV, the peak shape shift shows a peak centre at a lower binding energy; this change is consistent with the formation of metallic zinc, and is in agreement with the SEM images in Figure 2 which show damaged nanosheets at these acceleration voltages.
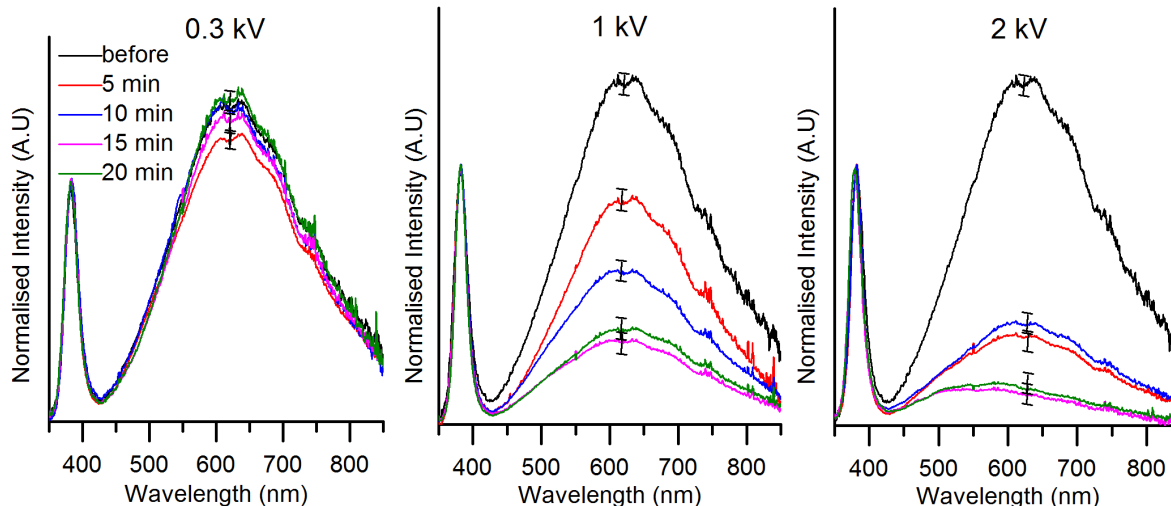
Figure 5: PL Spectra for ZnO nanosheets with different powers and time of argon bombardment. Error bar show standard deviation at 625 nm.

PL was carried out to characterise changes in the defect chemistry with each spectrum normalised to the near band edge (NBE) peak, shown in Figure 5. Before argon bombardment, the NBE peak was centred at 381.3 nm and the deep level emission (DLE) peak in the range of 400- 850 nm and shape of the DLE peaks is agreement with our previous work [7, 13]. There has been great debate in the literature over the origins of the constituent components of the DLE peak and defects in ZnO as a whole. These debates centre around the role of zinc and oxygen vacancies and interstitials as well as hydrogen impurities and density of states due to confinement and how the nature of the defects affect the conduction mechanisms [24-37]. As there is no consensus on the exact position and contribution of these components, the following discussion will focus on the overall changes in relative intensity of the DLE peak.

Argon bombardment at 0.3 kV did not alter the PL spectra, with both the NBE peak remaining centred at 381.3 nm for all time durations of bombardment. There were some variations in the relative intensities of the DLE peak but these were within the variation of the measurements and therefore not considered to be significant as the error bars overlap. Argon bombardment at 1kV also did not result in any measurable change to the position of the NBE peak. However, it was observed that the relative intensity of the DLE peak decreased with increased duration of bombardment. The spectra for the samples bombarded for 15 and 20 min do no statistically differ from each other as shown by the overlapping error bars. Our previous work [13] showed that using similar argon bombardment conditions stripped the

surface of ZnO nanorods, and the SEM images in Figure 2 also indicate that the surface of the nanosheets are stripped. Since the normalised DLE peak reduced with argon bombardment duration, it suggests that the defects that cause the DLE peak are mainly situated at the near surface and are removed when the near surface is stripped.

Argon bombardment at 2 kV for 5 and 10 minutes reduced the relative intensity of the DLE, with the unchanged peak shape and the position of the NBE peak did not shift during bombardment. Bombardment for 15 and 20 minutes further reduced the intensity of the DLE peak relative to the NBE peak, and again they did not significantly differ from each other. However as the Figure 2 shows, the nanosheets are damaged to a point where the surface is not clear therefore it is not possible to comment on the defect distribution for these samples. The position of the NBE peaks also shifted to 378.4 nm.
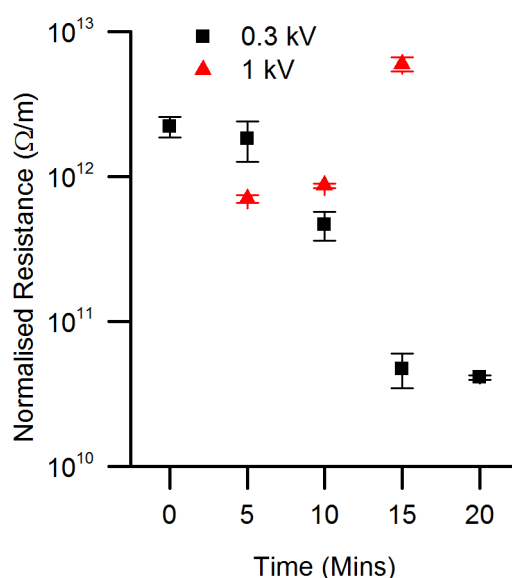
Figure 6. Graph of normalised resistance against duration of argon bombardment. Error bars show the standard error.

To assess the effects of argon bombardment on the transport properties of the ZnO nanosheets, nanoscale two-point probe was used to perform I-V measurements; the normalised resistance at +1 V is plotted against argon bombardment duration in Figure 6. Normalised resistance was calculated using the average of the measured resistances of the nanosheets divided by probe separation. Figure S2 in the supplemental information show SEM images of typical probe placements. The samples bombarded at 2 kV and 1 kV for 20

minutes were not characterised as the SEM images showed damage to the nanostructures that would create inconsistent results.

The average normalised resistance before argon bombardment was 2.22×10^{12} Ωm^{-1}. Argon bombardment at 0.3 kV for 20 mins caused a the normalised resistance to reduce to 4.12 $\times 10^{10}$ Ωm^{-1}, although it should be noted that the difference between 15 minutes and 20 minutes is not statistically significant. These results are in agreement with our previous work [13], which attributed the effect to surface cleaning.

Argon bombardment at 1 kV for 5 mins caused the normalised resistance to drop to 7.01×10^{11} Ωm^{-1}, however, further bombardment caused the resistance to increase, with the normalised resistance after 15 mins increasing to 5.96×10^{12} Ωm^{-1}. Again, this is in agreement with our previous work [13], which attributed this effect to the removal of defects resulting in a reduction in the number of charge carriers by stripping the surface of the nanostructure.

Figure 7 shows an I-V curve normalised to the current measured at +2 V for a typical nanosheet after bombardment for 20mins at 0.3 kV ("cleaned"), and bombarded at 1 kV for 15min ("stripped"). It was observed that the I-V curves measured before and after 0.3 kV bombardment were slightly rectifying in character, indicating that the tungsten probes made a Schottky contact to the nanosheets. A linear fit was used to quantify a typical cleaned I-V curve and the R^2 value was calculated to be 0.9917. However, the stripped I-V curve was more rectifying in character and the R^2 of a typical curve was calculated to be 0.9509. This is in agreement with our work on ZnO [13], which showed that this effect is a result of surface charge being removed from the ZnO nanosheets by a reduction in donor states. Removal of these defects resulted in increased band bending at the boundary between the probe and the material surface, yielding a more rectifying contact. It should be noted that the reduction in the normalised DLE peak indicates that all defects have reduced. This includes acceptor/p-type defects as well as n type defects, however, it is known that ZnO is naturally n-type therefore any reduction in acceptor defects has a minimal effect on the conduction mechanism when compared to a reduction in donor/ n-type defects [37]. It is noted that the contact made to the "cleaned" nanosheets is more rectifying than that made to "cleaned" nanorods in our previous work. We attribute this to the nanorods having a larger normalised defect peak, which was 2.5 times the intensity of the NBE peak, which corresponds to a

higher concentration of donor states at the surface, in turn resulting in a lower degree of band bending at the interface with the tungsten probe.
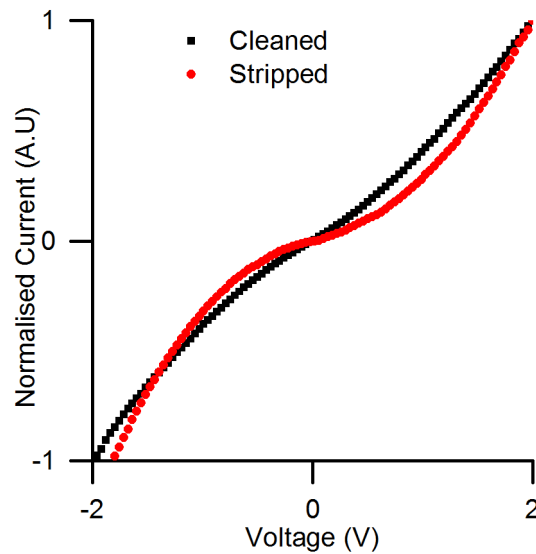
Figure 7. Graph of normalised current against voltage for a typical "cleaned" ZnO nanosheets and a typical "stripped" nanosheet.

Conclusion

ZnO nanosheets have been treated with increasing doses, by both power and time, of argon bombardment and the resulting changes in the electrical transport and defect chemistry have been measured experimentally using nanoscale two-point probe, XPS, PL and SEM. Low-powered, 0.3 kV doses of argon bombardment removed surface contamination without changing the defect chemistry. It was found that at least 15 minutes of treatment was needed to remove surface contamination and to reduce the resistance measured to a minimum, two orders of magnitude lower than before treatment.

Higher-energy bombardment at 1 kV resulted in surface stripping of the ZnO nanosheets, with 20 mins of bombardment causing holes to appear in the nanosheet structures. As the surface was stripped, the PL defect concentration reduced and the measured resistance increased. The reduction in defects resulted in less surface charge due to the removal of donor states causing increased band bending at the contact. Argon bombardment at 2 kV caused significant damage to the nanosheets, making it impossible to carry out reliable conductivity measurements.

The work presented herein indicates that removing surface contamination with a low-energy dose of argon bombardment results in more reproducible, lower resistance contacts without altering the defect chemistry. Our work also shows that the contact type can be controlled by selectively surface-stripping ZnO nanosheets with higher-energy doses of argon bombardment. The controlled removal of the defects and the ability to control the conduction/donor concentration of the nanostructure allows for enhancement of the sensitivity of devices such as gas sensors [4] and more efficient solar cells [6]. The work also indicates a possibility of controlling doping concentration within layers of the same nanostructure without the need for dopant implantation, which may be achieved by exposing only one side of the nanostructure to bombardment.

The results presented in this investigation agree with our previous work on ZnO nanorods. Within that study, it was found that defect states are concentrated in the surface of nanostructures even if they are polycrystalline in nature. It should be noted that the polycrystalline structure of ZnO nanosheets is more susceptible to damage from argon bombardment than single crystal ZnO nanorods, and that nanosheets appear to have a lower concentration of defects, which can result in a more rectifying contact.

References

[1]   Cheng H, Cheng J, Zhang Y and Wang Q-M 2007 Large-scale fabrication of ZnO micro-and nano-structures by microwave thermal evaporation deposition *Journal of Crystal Growth* **299** 34-40

[2]   Schmidt-Mende L and MacManus-Driscoll J L 2007 ZnO - nanostructures, defects, and devices *Materials Today* **10** 40-8

[3]   Tarat A, Majithia R, Brown R A, Penny M W, Meissner K E and Maffeis T G G 2012 Nanocrystalline ZnO obtained from pyrolytic decomposition of layered basic zinc acetate: Comparison between conventional and microwave oven growth*20-23 Aug. 2012)* p 1-5

[4]   Jones D R and Maffeïs T G G 2015 Analysis of the kinetics of surface reactions on a zinc oxide nanosheet-based carbon monoxide sensor using an Eley–Rideal model *Sensors and Actuators B: Chemical* **218** 16-24

[5]   Tarat A, Majithia R, Brown R, Penny M and Meissner K 2012 Synthesis of nanocrystalline ZnO nanobelts via pyrolytic decomposition of zinc acetate nanobelts and their gas sensing behavior *Surf Sci* **606** 715 - 21

[6]   Tarat A, Nettle C, Bryant D T J, Jones D, Penny M, Brown R, Majitha R, Meissner K and Maffeis T G G 2014 Microwave-assisted synthesis of layered basic zinc acetate nanosheets and their thermal decomposition into nanocrystalline ZnO *Nanoscale Research Letters* **9** 11

[7]   Barnett C, Smith N, Jones D, Maffeis T G and Cobley R 2015 Effects of Vacuum Annealing on the Conduction Characteristics of ZnO Nanosheets *Nanoscale Res. Lett.* **10** 1-6

[8]   Law J B K and Thong J T L 2008 Improving the NH 3 gas sensitivity of ZnO nanowire sensors by reducing the carrier concentration *Nanotechnology* **19** 205502

[9]   Ra H W, Khan R, Kim J T, Kang B R, Bai K H and Im Y H 2009 Effects of surface modification of the individual ZnO nanowire with oxygen plasma treatment *Materials Letters* **63** 2516-9

[10]   Ra H-W and Im Y-H 2008 Effect of chemically reactive species on properties of ZnO nanowires exposed to oxygen and hydrogen plasma *Nanotechnology* **19** 485710

[11]   Ra H-W, Choi K S, Ok C W, Jo S Y, Bai K H and Im Y H 2008 Ion bombardment effects on ZnO nanowires during plasma treatment *APPLIED PHYSICS LETTERS* **93** -

[12]   Dulub O, Boatner L A and Diebold U 2002 STM study of the geometric and electronic structure of ZnO(0001)-Zn, (000-1)-O, (10-10), and (11-20) surfaces *Surf. Sci.* **519** 201-17

[13]   Barnett C J, Kryvchenkova O, Smith N A, Kelleher L, Maffeis T G G and Cobley R J 2015 The effects of surface stripping ZnO nanorods with argon bombardment *Nanotechnol.* **26** 415701

[14]   Barnett C J, Kryvchenkova O, Wilson L S J, Maffeis T G G, Kalna K and Cobley R J 2015 The role of probe oxide in local surface conductivity measurements *J. Appl. Phys.* **117** 174306

[15]   Cobley R J, Brown R A, Barnett C J, Maffeis T G G and Penny M W 2013 Quantitative analysis of annealed scanning probe tips using energy dispersive x-ray spectroscopy *Appl. Phys. Lett.* **102**

[16]   Smith N A, Lord A M, Evans J E, Barnett C J, Cobley R J and Wilks S P 2015 Forming reproducible non-lithographic nanocontacts to assess the effect of contact compressive strain in nanomaterials *Semicond. Sci. Technol.*

[17]   Gao Y K, Traeger F, Shekhah O, Idriss H and Wöll C 2009 Probing the interaction of the amino acid alanine with the surface of ZnO *Journal of Colloid and Interface Science* **338** 16-21

[18]   Heinhold R, Cooil S P, Evans D A and Allen M W 2014 Stability of the Surface Electron Accumulation Layers on the Nonpolar (10Ī0) and (11Ż0) Faces of ZnO *The Journal of Physical Chemistry C* **118** 24575-82

[19]   Byrne D, McGlynn E, Henry M O, Kumar K and Hughes G 2010 A novel, substrate independent three-step process for the growth of uniform ZnO nanorod arrays *Thin Solid Films* **518** 4489-92

[20]   Crist B V 2005 PDF Handbooks of Monochromatic XPS Spectra Volume 2 *Pure Binary Oxides*

[21]   Maffeis T G G, Penny M W, Castaing A, Guy O J and Wilks S P 2012 XPS investigation of vacuum annealed vertically aligned ultralong ZnO nanowires *Surf. Sci.* **606** 99-103

[22]   Barnett C J, Castaing A, Jones D R, R. L A, Jenkins L J, Cobley R J and Maffeis T G G 2017 XPS investigation of titanium contact formation to ZnO nanowires *Nanotechnology* **28** 085301

[23]   Lau W M, Bello I, Huang L J, Feng X, Vos M and Mitchell I V 1993 Argon incorporation in Si(100) by ion bombardment at 15–100 eV *J. Appl. Phys.* **74** 7101-6

[24]   Wang M, Zhou Y, Zhang Y, Jung Kim E, Hong Hahn S and Gie Seong S 2012 Near-infrared photoluminescence from ZnO *APPLIED PHYSICS LETTERS* **100** 101906

[25]   Xu C, Chun J and Kimb D E 2007 Electrical properties and near band edge emission of Bi-doped ZnO nanowires *APPLIED PHYSICS LETTERS* **90** 1-3

[26]   Yang Y, Yan H, Fu Z, Yang B, Xia L, Xu Y, Zuo J and Li F 2006 Photoluminescence and Raman studies of electrochemically as-grown and annealed ZnO films *Solid State Communications* **138** 521-5

[27]   Lima S A M, Sigoli F A, Jafelicci Jr M and Davolos M R 2001 Luminescent properties and lattice defects correlation on zinc oxide *International Journal of Inorganic Materials* **3** 749-54

[28]   Lin B, Fu Z and Jia Y 2001 Green luminescent center in undoped zinc oxide films deposited on silicon substrates *APPLIED PHYSICS LETTERS* **79** 943-5

[29]   Liao Z-M, Zhang H-Z, Zhou Y-B, Xu J, Zhang J-M and Yu D-P 2008 Surface effects on
         photoluminescence of single ZnO nanowires *Physics Letters A* **372** 4505-9
[30]   Heo Y W, Norton D P and Pearton S J 2005 Origin of green luminescence in ZnO thin film
         grown by molecular-beam epitaxy *Journal of Applied Physics* **98** 073502
[31]   Janotti A and Van de Walle C G 2005 Oxygen vacancies in ZnO *APPLIED PHYSICS LETTERS* **87** -
[32]   Wei X Q, Man B Y, Liu M, Xue C S, Zhuang H Z and Yang C 2007 Blue luminescent centers and
         microstructural evaluation by XPS and Raman in ZnO thin films annealed in vacuum, N2 and
         O2 *Physica B: Condensed Matter* **388** 145-52
[33]   Xu P S, Sun Y M, Shi C S, Xu F Q and Pan H B 2003 The electronic structure and spectral
         properties of ZnO and its defects *Nuclear Instruments and Methods in Physics Research
         Section B: Beam Interactions with Materials and Atoms* **199** 286-90
[34]   Lijie L 2017 On the double-band luminescence of ZnO nanoparticles *EPL (Europhysics Letters)*
         117 67005
[35]   Janotti A and Van de Walle C G 2007 Native point defects in ZnO *Physical Review B* **76**
         165202
[36]   Fumiyasu O, Minseok C, Atsushi T and Isao T 2011 Point defects in ZnO: an approach from
         first principles *Science and Technology of Advanced Materials* **12** 034302
[37]   McCluskey M D and Jokela S J 2009 Defects in ZnO *Journal of Applied Physics* **106** -